Synthesis and Degradation of Nucleic Acid Components by Formamide and Cosmic Dust Analogues

Raffaele Saladino,*[a] Claudia Crestini,[b] Veronica Neri,[a] John R. Brucato,[c] Luigi Colangeli,[c] Fabiana Ciciriello,[d] Ernesto Di Mauro,*[e] and Giovanna Costanzo[d]

We show the unprecedented one-pot synthesis of a large suite of pyrimidines (including cytosine and uracil) and purines from formamide in the presence of cosmic-dust analogues (CDAs) of olivines. Since the major problem in the origin of informational macromolecules is the instability of their precursors, we also investigate the stabilizing effect of CDAs on the intrinsic instability of oligonucleotides in formamide.

Introduction

All strategies for the prebiotic synthesis of nucleobases assume the adequate availability[1] of the presumptive precursors, such as hydrogen cyanide, formaldehyde, ammonium cyanide, and cyanoacetylene. The step-up from these precursors or from mixtures of simple gases to more complex compounds was shown to occur under a variety of conditions: electric discharge, UV irradiation, ion-irradiation heating, marine vents, carbon dioxide chemistry on pyrite clusters.[2–6] However, no reliable single physicochemical scenario[7] for the prebiotic Earth or for plausible pristine synthesis of these bases is yet available. No physicochemical consensus exists for the necessary simultaneous availability[8–10] of all or a large number of the nucleic acid precursors, particularly for pyrimidines[11] and sugars.[12] Thus, we have explored the possibility that formamide might provide the chemical frame for such a general unitary picture.

Formamide (NH_2COH) is active both in the synthesis of nucleobases[13,14] and in the selective degradation of DNA.[15] The condensation of formamide is catalyzed and modulated by several inorganic compounds and results in the production of purine and pyrimidine nucleobases, and purine acyclonucleosides (Table 1).[16,17] The role of these catalysts is not limited to the increase of reaction yields, but also provides selectivity.[16–18] Since formamide degrades DNA,[15] we have studied both the formamide-based synthesis and degradative pathways of nucleic acid components under comparable conditions. This coupled approach is necessary because in any physicochemical scenario that deals with the origin of life, the *stability* of the precursor molecules is a major concern.[19,20]

Here we describe the role of a wide range of olivines (from fayalite to forsterite) in i) the synthesis of purine and pyrimidine derivatives from formamide and ii) the formamide induced degradation of nucleic acid components. Since formamide[21,22] and olivines[23] are sizeable components of cosmic dust, the effect of olivines prepared in the form of cosmic-dust analogues (CDAs) was analyzed.[24]

Results

Based on results from space missions, space and ground-based observations, and laboratory analyses of interplanetary dust particles (IDPs)[23] "fluffy" grains of amorphous olivines were synthesized in the laboratory (see Experimental Section). They were synthesized as CDAs in order to reproduce the chemical composition and morphology of silicate dusts expected in different astronomical environments.[24]

[a] *Prof. R. Saladino, Dr. V. Neri*
Dipartimento A.B.A.C., Università della Tuscia
Via San Camillo De Lellis, 01100 Viterbo (Italy)
Fax: (+39) 0761-357-242
E-mail: saladino@unitus.it

[b] *Dr. C. Crestini*
Dipartimento di Scienze e Tecnologie Chimiche
Università "Tor Vergata"
00133 Rome (Italy)

[c] *Dr. J. R. Brucato, Prof. L. Colangeli*
INAF–Osservatorio Astronomico di Capodimonte
Via Moiariello 16, 80131 Naples (Italy)

[d] *Dr. F. Ciciriello, Dr. G. Costanzo*
Istituto di Biologia e Patologia Molecolari, CNR
00185 Rome (Italy)

[e] *Prof. E. Di Mauro*
Fondazione "Istituto Pasteur, Fondazione Cenci Bolognetti"
c/o Dipartimento di Genetica e Biologia Molecolare
Università "La Sapienza"
P.le Aldo Moro 5, 00185 Roma (Italy)
Fax: (+39) 06-4991-2880
E-mail: ernesto.dimauro@uniroma1.it

Supporting information for this article is available on the WWW under http://www.chembiochem.org or from the author.

  DOI: 10.1002/cbic.200500035 *ChemBioChem* **2005**, *6*, 1368 – 1374

Table 1. Catalyzed synthesis of nucleic acid components from formamide.

Product	Catalyst: Silica	Alumina	Kaolin	Zeolite	$CaCO_3$	KP-10[b]	K-30[b]	KSF[b]	Al-PILC[b]	TiO_2
purine	+[a]	+++++	+++++	+++++	+++++	++++	+	++++	+++	+++
adenine	+	+	0	+	0	++	++++	+++	+	++
hypoxanthine	0	0	0	0	0	+	0	+	+	0
N9-formylpurine	0	0	0	0	0	+++	++++	+	+	+++
N,*N*-diformyladenine	0	0	0	0	0	0	0	0	0	+
acyclonucleosides	0	0	0	0	0	0	0	0	0	++
cytosine	+	+	0	+	0	+++	+++	+++	+++	+
hydroxypyrimidine	+	+	+	+	0	0	0	0	0	0
uracil	0	0	0	0	0	+	+	+	+	0
thymine	0	0	0	0	0	0	0	0	0	+
hydroxymethyluracil	0	0	0	0	0	0	0	0	0	+
AICA	0	0	0	0	0	0	0	++++	+++	0
FAICA	0	0	0	0	0	++	++++	+++	+	0

[a] mg of product per gram of formamide. +: 0.1–5.0 mg; ++: 5–10 mg; +++: 10–20 mg; ++++: 20–40 mg; +++++: >40 mg. [b] Activated montmorillonites. AICA: 5-aminoimidazole-4-carboxamide; FAICA: 5-formamidoimidazole-4-carboxamide. Data from ref. [16] (Silica, Alumina, Kaolin, Zeolite, $CaCO_3$), [18] (KP10, K30, KSF, Al-PILC), [17] (TiO_2).

CDAs were produced by fast condensation of target vaporized materials by high-energy Nd:YAG laser ablation. Laser targets were oxide mixtures (SiO_2, MgO, FeO). Each component was weighed in order to give the exact stoichiometric composition of olivines with different magnesium and iron content: fayalite Fe_2SiO_4 (sample A), $Mg_{0.5}Fe_{1.5}SiO_4$ (sample B), olivine $MgFeSiO_4$ (sample C), $Mg_{1.5}Fe_{0.5}SiO_4$ (sample D), and forsterite Mg_2SiO_4 (sample E). Preparation, morphology, elemental chemical composition, and spectroscopy characterization of the samples are given in the Experimental Section and ref. [24].

Synthetic catalysis with CDAs

To evaluate the catalytic effects of CDAs on the prebiotic synthesis of nucleobases, several experiments were performed by heating neat formamide (**1**; Scheme 1) in the presence of the appropriate compound. Reference reactions in the presence of parent olivines were also performed. Products were characterized by gas-chromatography mass-spectrometry (GC-MS) analysis, after derivatization with bis(trimethylsilyl)acetamide, and by ^1H and ^{13}C NMR analysis (Scheme 1 and Table 2). Irrespective of the CDA used in the formamide condensation, a suite of pyrimidine derivatives, namely 4-(3*H*)-pyrimidinone (or 4-hydroxypyrimidine; **2**), cytosine (**3**), and uracil (**4**) were obtained in acceptable yield. 4-(3*H*)-Pyrimidinone was the most abundant product (Table 2, entries 2–5). 4-(3*H*)-Pyrimidinone was among the most abundant pyrimidines recovered from the Murchison meteorite.[25,26] Low amounts of purine **5**, urea (**6**), and 5,6-dihydrouracil (**7**) were also detected. Compound **7** was only obtained with olivine $Mg_{0.5}Fe_{1.5}SiO_4$ (Table 2, entry 9). Urea is a well known prebiotic precursor for both purine and pyrimidine nucleobases, and might be formed by formamide degradation of pyrimidine nucleobases, even though its direct formation from formamide cannot be ruled out.[14]

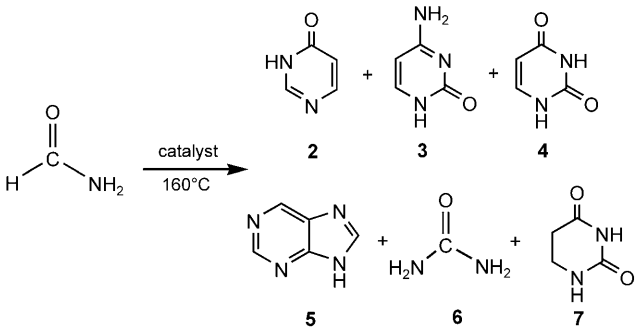

Scheme 1. Condensation of formamide in the presence of CDAs.

The products described above accounted for about 90% of the total yield. The additional components were not identified due to their small quantities, with the exception of one compound whose mass spectrum can be interpreted as being that of a deoxyribose derivative. (This compound is currently undergoing further analysis.)

The condensation of formamide performed in the absence of olivine derivatives yielded purine as the only recovered product (Table 2, entry 1). Purine derivatives, adenine in particular, are usually obtained as the most abundant products during prebiotic syntheses from simple one-carbon-atom precursors, such as, HCN and formamide. Furthermore, we observe that CDAs are specific and selective microenvironments for the formation of pyrimidine derivatives, including cytosine and uracil; uracil could be formed by cytosine hydrolysis. CDAs were found to be more efficient catalysts than their parent compounds (e.g., Table 2 entry 3 vs. 8 and entry 5 vs. 10). These data suggest that IDPs might be favorable microenvironments for the prebiotic synthesis of pyrimidine nucleobases that are not easily obtained under terrestrial conditions. Moreover, the elemental composition of CDAs was found to be an important parameter for the selectivity of the reaction. For example: fayalite (sample A) and $Mg_{0.5}Fe_{1.5}SiO_4$ (sample B) CDAs, characterized by the absence or presence of low amounts of magnesium ions, yielded high amounts of 4-(3*H*)-pyrimidinone, cytosine, and uracil (Table 2, entries 5 and 4). However, forster-

Table 2. Quantitative profile of the products obtained by formamide condensation in the presence of olivines and CDAs.

	Catalyst	Sample	Yield[b] Pyrimidinone (**2**)	Uracil (**3**)	Cytosine (**4**)	Purine (**5**)	Urea (**6**)	Dihydrouracil (**7**)
1	No catalyst		0	0	0	34.1	0	0
2	$MgFeSiO_4$*[a]	C	19[b]	2.4	19.6	0.3	0.1	0
3	$Mg_{1.5}Fe_{0.5}SiO_4$*[a]	D	19.5	0	32.3	0	0.1	0
4	$Mg_{0.5}Fe_{1.5}SiO_4$*[a]	B	72.6	2.1	22.5	0	0	0
5	Fe_2SiO_4*[a]	A	241	4.5	68.6	1.2	3.2	0
6	Mg_2SiO_4*[a]	E	0	0	0	0.7	1.0	0
7	$MgFeSiO_4$	C	5.2	0.8	4.7	0	0.2	0
8	$Mg_{1.5}Fe_{0.5}SiO_4$	D	9.9	0	0	0	0	0
9	$Mg_{0.5}Fe_{1.5}SiO_4$	B	3.7	2.2	7.0	0.2	0	4.2
10	Fe_2SiO_A	A	5.4	0	0	0	0	0
11	Mg_2SiO_4	E	0.13	0	0	0	0	0

[a] Cosmic dust analogues (CDAs). [b] Quantitative evaluations were performed by capillary gas-chromatography analysis as described in the Experimental Section. Because of the uncertainty of the number of formamide molecules involved in the synthesis of the recovered products the yields were calculated as mg of product formed per gram of formamide.

ite CDA, which is devoid of iron, did not yield pyrimidines (Table 2, entry 6).

Degradative catalysis by cosmic dust analogues

The decomposition of DNA and the degradation pathway of oligonucleotide-embedded purine and pyrimidine bases by formamide have been described.[13–15] The decreasing order of sensitivity to degradation is: purine, inosine, guanine > adenine > cytosine ≫ thymine, and the chemical mechanisms that are involved have been determined.[13,14] For purines, degradation occurs by nucleophilic attack in the C8 position, which leads to degradative opening of the imidazole ring.[13] For pyrimidines degradation occurs by nucleophilic attack in the C6 or in both the C4 and C6 positions.[14] Following degradation and removal of the heterocyclic base, the two reactive protons Hα and Hγ (Figure 1 A) are available for β-elimination reactions, which lead to 3′- and 5′-phosphodiester bond cleavage, respectively. The strength of Hα is higher than that of Hγ,[15] so that in a weak base such as formamide, the cleavage of the 3′-phosphodiester bond occurs preferentially to that at the 5′ end.[14,15] On 3′-labeled DNA molecules, the cleavage at the 5′ end is label-distal and is masked by the robust band generated at the 3′ label-proximal side.

This behavior provides an assay for the study of the effects of the DNA-backbone interaction with CDA olivines. An alteration of the standard cleavage reaction, caused by the interaction of the oligonucleotide backbone with the catalyst surface, is manifested as an intensity variation of the 3′ and/or 5′ bonds. This reveals the relative strength of the pentose Hα/Hγ protons (Figure 1 A).

The effect of CDA olivines on formamide degradation of polynucleotides was studied on homogeneous polymers that were embedded in mixed-sequence stretches. The complete analysis is described in the Supporting Information. Figure 1 B shows the degradation pattern of a 3′-labeled poly-A oligonucleotide with mixed-sequence terminal segments. The polynucleotide was treated with formamide in the absence or presence of the indicated amounts of untreated (lanes 1–6) or UV-laser ablated (lanes 7–12) CDA olivine. The effects of untreated olivine were alteration of the base selectivity of the formamide attack (i.e., cleavage at A's is much less inhibited than of the C's—see the mixed-sequence in the upper part of the gel); moderate alteration of the 3′/5′ cleavage ratio; overall protection as a function of increased concentration; sequestering of oligonucleotide at higher concentrations (lanes 5 and 6).

The olivines prepared as CDAs produce quite different effects (lanes 7–12): marked loss of base-cleavage selectivity even at low concentration (lane 8); strong alteration of the 3′/5′ cleavage ratio with marked increase of 5′ cleavage; weak protection effect. Figure 2 compares five different compounds (A–E) as a function of concentration. They were tested as untreated mixture of oxides (left panel) or as CDA compounds (right panel).

In summary, the effect of CDA olivines on DNA attack by formamide consists of the alteration of base selectivity (G > A > C ≫ T), and modification of the rate of β-elimination of Hα/Hγ protons.

Conclusion

Since prebiotic self-replicating molecules were a priori not supported by complex enzymatic systems, emergence of life must have been a robust phenomenon. We consider that the more common the precursors were, the simpler and more unitary must have been the chemistry involved; the more widespread the catalysts that provided selectivity and improvement in yields, the higher must have been the chances that information-bearing oligomers would form and replicate. This implies—among other polymerization-related requirements[12]—at least the simultaneous presence of purines and pyrimidines in comparable concentrations.

Such coexistence would obviously be favored by a single chemical frame for their synthesis and also by equilibrated synthesis/degradation rates. If a compound (i.e., adenine) were synthesized in higher amounts, its excessive concentration could have been compensated for by a higher degradation rate. Correspondingly, the scarce synthesis of thymine could have been compensated for by its higher resistance to degradation.[14–16] Taken together, the formamide-based unitary chemical frame for the synthesis of a complete suite of precursor bases (Tables 1 and 2) and their differential stabilities in formamide,[14–16] prevent a strong imbalance of precursor concentrations.[41] The availability of an equilibrated pool of precursors would have facilitated the initial synthetic processes. We thus propose that the initial unitary chemical frame was based on formamide chemistry.

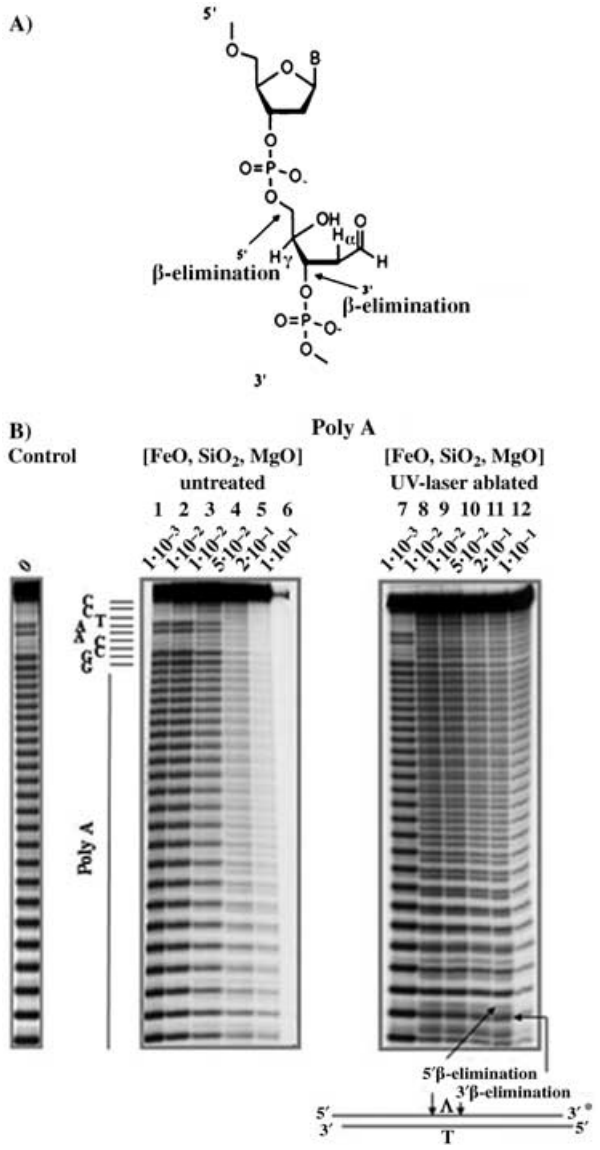

Figure 1. CDA olivines modify the degradative reactions of formamide on DNA. Degradation of a 3′-labeled 46-base long oligonucleotide containing a 30 bp poly-A stretch and mixed sequence termini (see Supporting Information for details). A) Cleavage of 3′ and 5′ phosphodiester bonds by amides. Schematic representation of the degradation of the sugar moiety that indicates the two different β-eliminations (see text). B) The reaction with formamide (110 °C, 20 min) was performed in the absence (control lane) or in the presence of untreated (lane 1–6) or of UV-LA (lanes 7–12) CDA olivine. The concentration of olivines in the reactions (mg mL^{-1}) are indicated at the top of each lane. The 3′ and 5′ β-elimination bands are shown schematically.

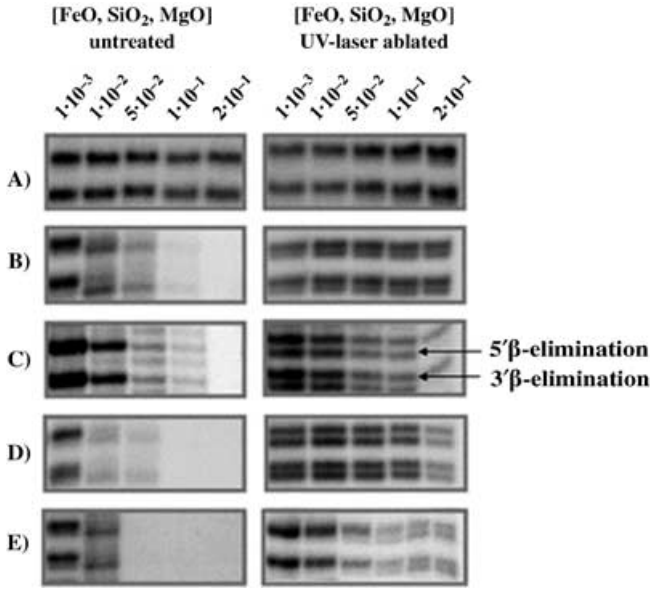

Figure 2. CDA olivines modify the degradative reactions of formamide on DNA. The effect of the range of chemically different olivines is described. A) Fayalite Fe_2SiO_4; B) $Mg_{0.5}Fe_{1.5}SiO_4$; C) olivine $MgFeSiO_4$; D) $Mg_{1.5}Fe_{0.5}SiO_4$; E) forsterite Mg_2SiO_4; see text for details. Experimental procedures were carried out as described for Figure 1. The bands correspond to positions 15 (upper band) and 16 (lower band) of the poly-A region.

Formamide, which is a product of HCN hydrolysis, is stable in liquid even above 200 °C and shows limited azeotropic effects.[27] Its role as an imidazole and oxazole precursor has been described.[28] Formamide-based reactions that yield nucleobases result in different populations of products that mostly consists of purines but also pyrimidines and acyclonucleosides.[16–18] The composition of these depends on the catalyst present. $CaCO_3$, silica, alumina, kaolin, zeolites, TiO_2, and montmorillonite clays[16–18] all favor the formation of purines.

Here we show that CDA olivines favor formamide condensation into pyrimidines and actively decrease formamide-based oligonucleotide instability.

Formamide is among the organic molecules present in the interstellar medium,[21,22] as are olivines.[23] The detection of purines and pyrimidines in meteorites (of which Murchison is only one instance)[25,26] provides a clear example of extraterrestrial syntheses and poses the question of their origin. Given that large amounts of organic molecules were deposited on the primitive Earth by asteroids, comets, meteorites, and IDPs,[7,21] the formamide/olivines substrate/catalyst combination described here provides a plausible example of the chemical forces and possibilities in action that could kick-start the phenomenon of primordial polymerizations. This process had to be robust enough to allow neo-Darwinian selection, and was certainly not based on elaborate precursors and rare catalysts.

The experiments reported do not allow firm conclusions on the possible early-Earth environment(s) in which the described catalyses could have taken place. However, the fact that explored active synthetic processes do take place at high temperature (110–160 °C) and under dry conditions suggests volcanic environments. This is in agreement with the results of the analysis of catalytic property of montmorillonites on prebiotic syntheses. Given that there is no a priori reason to assume morphological and chemical instability of cosmic dust particles after arriving on early Earth, the observed catalytic properties of CDAs and volcanic environments are not in contrast. The properties of CDAs at low temperatures and in a photochemistry frame (or in general under space-like conditions) deserve further studies.

Experimental Section

Preparation of UV-laser ablated (UV-LA) olivines: Principal sites of cosmic dust formation are envelopes of giant stars that belong to the asymptotic branch (AGB) and supernovae (SN).[29–30] Once formed, grains are injected in the interstellar medium (ISM) and collected during planetary system formation as building blocks of large bodies. Based on results from space missions,[31] space and ground-based observations,[23,32,33] and laboratory analyses of IDPs[34–37] "fluffy" grains of amorphous olivines were synthesized in the laboratory as CDAs with the aim of reflecting the chemical composition and morphology of silicate dust expected in different astronomical environments.[24]

CDAs were produced by fast condensation of vaporized target by high energy Nd:YAG laser ablation. Laser targets were oxide mixtures (SiO_2, MgO, FeO). Each component was weighed in order to obtain the exact stoichiometric composition of olivines with different magnesium and iron content: pure fayalite Fe_2SiO_4 (sample A), $Mg_{0.5}Fe_{1.5}SiO_4$ (sample B), $MgFeSiO_4$ (sample C), $Mg_{1.5}Fe_{0.5}SiO_4$ (sample D), and pure forsterite Mg_2SiO_4 (sample E). The targets were prepared by pressing the oxide mixtures at 15 tons to produce pellets 13 mm in diameter and few millimeters in thickness. Surelite II laser (fundamental wavelength at 1064 nm) equipped with two crystals was used to obtain forth harmonics at UV wavelength of 266 nm. An optical set-up selects and focuses the UV laser beam on the target to give a power density of $10^9\,W\,cm^{-2}$ on a spot 2 mm in diameter. The target is mounted inside a vaporization chamber designed to work at different gas pressures. In this experiment, the O_2 atmosphere was 10 mbar. The oxidative atmosphere prevents iron segregation that could form grains of pure iron metal during condensation. Moreover, the presence of an atmosphere inside the evaporation chamber causes hot atoms of laser plume to lose their energy by collision with the cold O_2 atoms. The high expansion velocity (10^4–$10^5\,cm\,s^{-1}$) of the hot gas in the laser plume and the collision-cooling mechanism (collision mean free path of 10^{-4} cm for O_2 gas at 10 mbar) favor the supersaturation of the vapor. These are the appropriate conditions to induce condensation. The particles produced have a size distribution and average size that depend on the pressure and molecular weight of the cooling gas and the laser power density.[38] Due to the faster expansion of the laser-produced vapor plume in a lower pressure atmosphere, the particle sizes decrease as the gas pressure inside the evaporation chamber is reduced. The solid samples are then collected on appropriate substrates at a distance of about 3 cm from the target.

The morphological characterization of the samples was performed with a field emission scanning electron microscope (FESEM; Stereoscan FE360) with a spatial resolution of 2 nm. To prepare samples for FESEM analysis, laser-produced grains were collected on silicon substrate that was exposed to the dust flux during laser ablation.

The samples were coated with a Cr film in order to avoid charge build up under the electron beam of the microscope and obtain the best space resolution. Images at different magnifications were acquired from different regions of each sample.

The chemical composition of the samples was studied by means of an energy dispersive X-ray (EDX) detection system that was linked to the FESEM. For this kind of analysis grains were uniformly deposited on a carbon stub. The EDX spectra were acquired from five different regions and the average elemental content was measured. Appropriate software was used to evaluate the mass concentration of the elements by comparing X-ray spectra with those of standard samples.

Spectroscopic measurements were performed in the mid-infrared region in transmission. Dust samples were embedded in KBr and pressed into pellets. Spectra were acquired at a resolution of $2\,cm^{-1}$ by means of a FTIR interferometer (Bruker Equinox 55) and absorbance, A, was calculated in terms of transmittance, T, with the equation: $A = -\ln T$.

Characterization of UV-LA CDA olivines: The scanning electron micrographs showed that CDAs are very "fluffy" samples that are characterized by the presence of two morphological classes: 1) chain-like agglomerates of small spheroidal grains; and 2) isolated spheres (Figure 3). The shape and sizes observed were typical of fast vapor condensation and liquid coalescence processes.[39,40] The spheroidal shape of small grains (class 1) is the result of the Gibbs–Wulff criterion,[41] which predicts that the grain shape is achieved when $\sum_i \xi_i A_i$ is at a minimum; ξ_i is the specific surface free energy of the ith grain face, and A_i is the area. Under our experimental conditions, the surface migration time, t_s, of the impinged atoms is greater than the time interval, t_i, between two consecutive arrivals of atoms from the vapor phase onto the grain surface. Thus, atoms do not have sufficient time to gain a crystalline structure and amorphous spherical grains are formed (Figure 3).

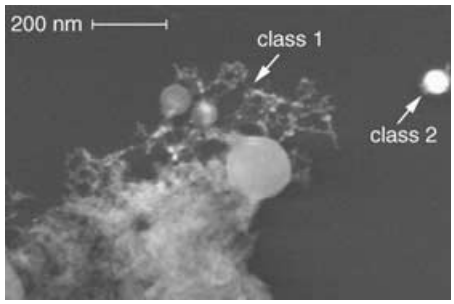

Figure 3. FESEM micrograph of CDA sample E (Mg_2SiO_4) deposited onto silicon wafer. Two morphological classes are visible: 1) chain-like agglomerates of small spheroidal grains; and 2) isolated spheres.

A fraction of the UV-LA particles can behave like a liquid and coalesce, thereby combining their volumes. This postcondensation process is responsible for the presence of isolated spheres (class 2). Further evidence for active postcondensation-coalescence process can be obtained by the analysis of CDA grain-size distribution. The good agreement with the log–normal distribution function, which was derived with the statistical theory of coalescence of spherical grains,[40] indicates that coalescence is also an active process in the laser-ablation technique used in this work.

The concentrations of CDA elements show a systematic decrease between the target and the condensed samples. This is observed when samples with fluffy textures are measured, because the electron beam crosses a smaller volume fraction of material and detects a lower X-ray signal. Even if this can affect the evaluation of the amount of oxides, the stoichiometry of the samples remains unchanged within error.

Absorbance of CDA sample E (Mg_2SiO_4), prepared as laser target and after laser ablation, is reported in Figure 4. The spectrum of the laser target shows the presence of all the bands of the oxides

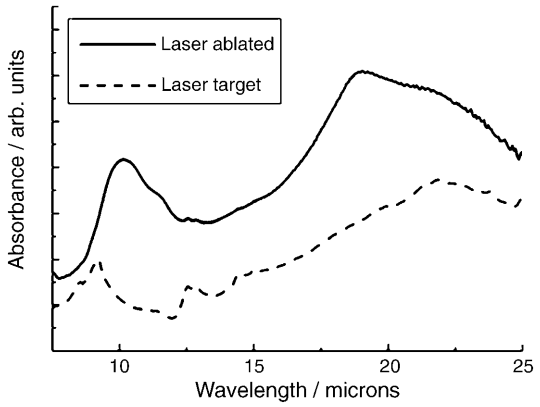

Figure 4. Absorbance in arbitrary units of CDA sample E (Mg_2SiO_4) prepared as laser target (dashed line) and after laser ablation (solid line). The presence of two broad and smooth bands at 10.1 and 19.1 indicate the chemical transformation of SiO_2 and MgO oxides in amorphous olivine.

that were used for target preparation. In particular the bands at 8.5, 9.2, 12.5, and 21.3 μm of SiO_2 and 12.5, 12.8, 14.5, 15.0, and 21.8 μm of MgO are presented. After laser ablation, two broad and smooth bands at 10.1 and 19.1 μm of amorphous olivine are observed; these bands are due to stretching and bending of silicon–oxygen bonds, respectively. The presence of weak target oxide bands observed in the laser-ablated spectrum, imply that small fractions of particles are ejected from the target as pure oxides without being involved in silicate-formation reactions.

Formamide-based synthesis: Formamide (>99%; Fluka) and 6-methoxypurine (Aldrich) were used without further purification. GC analysis and mass spectra were performed on an Hewlett–Packard 5890II gas chromatograph and a Shimadzu GC-MS QP5050A equipped with an Alltech® AT-20 column (0.25 mm, 30 m). ^{1}H and ^{13}C NMR spectra were recorded on a Bruker (200 MHz) spectrometer and are reported in δ = value. Microanalyses were performed with a C. Erba 1106 analyzer. Chromatographic purifications were performed on columns packed with Merck silica gel, 230–400 mesh for flash technique.

Formamide condensation: Formamide (5.7 g, 5 mL, 0.12 mmol) was heated at 160 °C for 48 h in the presence of CDAs of olivines: fayalite Fe_2SiO_4 (sample A), $Mg_{0.5}Fe_{1.5}SiO_4$ (sample B), olivine MgFeSiO$_4$ (sample C), $Mg_{1.5}Fe_{0.5}SiO_4$ (sample D), and forsterite Mg_2SiO_4 (sample E; 2% *w*/*w*). Reference experiments were performed with the parent olivines under similar experimental conditions.

The reaction mixture was allowed to cool, filtered to remove the catalyst, and evaporated under high vacuum. GC-MS of a portion of the crude reaction was performed after derivatization with *N*,*N*-bis(trimethylsilyl)acetamide by using an isothermal temperature profile of 100 °C for the first 2 min, followed by a 10 °C min^{-1} temperature gradient to 280 °C, and finally an isothermal period at 280 °C for 40 min. The injector temperature was 280 °C. Chromatography grade helium was used as the carrier gas. The fragmentation patterns were compared with those of authentic samples. 6-Methoxypurine was used as internal standard. The crude reaction mixture was also purified by flash chromatography ($CHCl_3$/CH_3OH 9:1). The structure of isolated products was confirmed with spectroscopic techniques and by comparison with commercial samples. Selected mass spectrometric data of compounds **2**–**7** are reported in Table 3.

Table 3. Selected mass spectrometric data of compounds **2**–**7**.

Products	*m*/*z* (%)
pyrimidinone (**2**)	96 (100) [*M*], 69 (31) [*M*−HCN], 53 (28) [*M*−NHCO]
cytosine (**3**)	111 (100) [*M*], 95 (20) [*M*−NH$_2$], 83 (28) [*M*−CO], 69 (45) [*M*−NCO], 41 (58) [*M*−HNCO−HCN]
uracil (**4**)	112 (100) [*M*], 69 (74) [*M*−HNCO], 42 (21) [*M*−HNCO−HCN]
purine (**5**)	120 (100) [*M*], 93 (37) [*M*−HCN], 86 (19) [*M*−2HCN]
urea (**6**)	60 (100) [*M*], 44 (32) [*M*−NH$_2$]
dihydrouracil (**7**)	114 (100) [*M*], 71 (64) [*M*−HNCO], 43 (21) [*M*−HNCO−HCN]

[a] Mass spectroscopy was performed with Hewlett–Packard 5971 mass-selective detector on a Hewlett–Packard 5890III gas chromatograph with an FID detector. Samples were analyzed after treatment with *N*,*N*-bis-trimethylsilylacetamide and pyridine.

Selected spectroscopic data for 4(3*H*)-pyrimidinone (**2**): m.p. 166–169 °C (EtOH); ^{1}H NMR ([D$_6$]DMSO) δ = 6.35 (d, *J* = 5.0 Hz, 1H; CH), 7.95 (d, *J* = 5.0 Hz, 1H; CH), 8.20 (s, 1H; CH), 12.8 (br s, 1H; NH); ^{13}C NMR ([D$_6$]DMSO) δ = 118.45 (CH), 145.10 (CH), 147.02 (CH), 163.33 (C); FTIR (Nujol) $\tilde{\nu}_{max}$ = 3460, 3300, 2890, 1680, 1600, 1475 cm^{-1}.

Preparation of oligonucleotides: The differential effects of metal oxides and olivines on the degradation of polynucleotides by formamide was studied on homogeneous polymers embedded in mixed-sequence stretches. The overall approach consisted of the analysis of the degradation products of two synthetic 2′-deoxyoligonucleotides. These were made of two short mixed-sequence ends (ten and six bases long at the 5′- and 3′-ends, respectively) and of a central 30-base-long homogeneous stretch of Gs, As, Cs, or Ts. The oligonucleotides used were:

Oli1: 5′-ACCTAACCGG[G]$_{30}$CCGGTT-3′
Oli2: 5′-ACCTAACCGG[A]$_{30}$CCGGTT-3′
Oli3: 5′-CCCGAACCGG[C]$_{30}$CCGGTT-3′
Oli4: 5′-CCCGAACCGG[T]$_{30}$CCGGTT-3′

These oligonucleotides were designed so as to be pair-wise complementary (i.e., Oli1 with Oli3, and Oli2 with Oli4). After annealing, the uncomplementary overhangs at the 5′ ends, each four nucleotides long, was used for selective labeling as described.[17] The degradation conditions used in this assay cause less than one hit per molecule, as shown by the regularity of the cleavage patterns and by the presence of a substantial amount of unreacted molecules.

Degradations of oligonucleotides by formamide in the presence of olivines: Each oligonucleotide (2 μg) was annealed with the same amount of its complementary oligo and labeled with [α^{32}P]dCTP (Oli2) or with [α^{32}P]dATP (Oli3). Labeling was performed by using T7 Sequenase (USBC-Amersham Biosciences), and the labeled oligo was purified on a 10% denaturing acrylamide gel (acrylamide/bisacrylamide 19:1). The polyacrylamide was removed by a NuncTrap probe purification column (Stratagene), and DNA (2 πmol; typically 300000 cpm) was processed for each sample. The DNA was ethanol precipitated, resuspended in formamide (5 μL; Fluka) and added to formamide (97%, 10 μL) that contained the indicated amounts of the appropriate olivine compound. After 20 min at 110 °C, a solution of tetrasodium pyrophosphate (final concentration 5×10^{-4} M; Sigma) was dissolved in water and made up to a final volume of 40 μL. The samples were vortexed for 1 min, then centrifuged at 13000 rpm for 20 min. The washed samples were combined, ethanol precipitated, resuspended in forma-

mide (5 μL) buffer, heated for 2 min at 95 °C, and loaded on a 16% denaturing polyacrylamide gel (19:1 acrylamide/bisacrylamide). For these methods see also refs. [16, 17].

Acknowledgements

We thank S. Inarta, E. Zona, and N. Staiano for technical assistance. This research was supported by the Italian Space Agency, Genomica Funzionale, BEMM, FIRB, and by MIUR COFIN 2003 "La catalisi dei metalli di transizione nello sviluppo di strategie sintetiche innovative di eterocicli".

Keywords: cosmic-dust analogues · nucleic acids · nucleobases · oligonucleotides · pyrimidines

[1] S. L. Miller, *Cold Spring Harbor Symp. Quant. Biol.* **1987**, *52*, 17 – 27.
[2] S. L. Miller, *Science* **1953**, *117*, 528 – 529.
[3] G. F. Joyce, *Nature* **1989**, *338*, 217 – 224.
[4] C. Huber, G. Wächtershäuser, *Science* **1997**, *276*, 245 – 247.
[5] G. Wächtershäuser, *Prog. Biophys. Mol. Biol.* **1992**, *58*, 85 – 201.
[6] P. S. Braterman, A. G. Cairns-Smith, R. W. Sloper, *Nature* **1983**, *303*, 163 – 164.
[7] C. F. Chyba, C. Sagan, *Nature* **1992**, *355*, 125 – 132.
[8] S. L. Miller, L. E. Orgel in *The Origins of Life on the Earth*, Prentice–Hall, New York, **1974**.
[9] W. Gilbert, *Nature* **1986**, *319*, 618.
[10] R. F. Gesteland, T. R. Cech, R. A. Atkins in *The RNA World*, 2nd ed., Cold Spring Harbor Laboratory, New York, **1998**.
[11] R. Shapiro, *Proc. Natl. Acad. Sci. USA* **1999**, *96*, 4396 – 4401.
[12] L. E. Orgel, *Trends Biochem. Sci.* **1998**, *23*, 491 – 495.
[13] R. Saladino, E. Mincione, C. Crestini, R. Negri, E. Di Mauro, G. Costanzo, *J. Am. Chem. Soc.* **1996**, *118*, 5615 – 5619.
[14] R. Saladino, C. Crestini, E. Mincione, G. Costanzo, E. Di Mauro, R. Negri, *Bioorg. Med. Chem.* **1997**, *5*, 2041 – 2048.
[15] R. Negri, G. Costanzo, R. Saladino, E. Di Mauro, *BioTechniques* **1996**, *21*, 910 – 917.
[16] R. Saladino, C. Crestini, G. Costanzo, R. Negri, E. Di Mauro, *Bioorg. Med. Chem.* **2001**, *9*, 1249 – 1253.
[17] R. Saladino, U. Ciambecchini, C. Crestini, G. Costanzo, R. Negri, E. Di Mauro, *ChemBioChem* **2003**, *4*, 514 – 521.
[18] R. Saladino, C. Crestini, U. Ciambecchini, F. Ciciriello, G. Costanzo, E. Di Mauro, *ChemBioChem* **2004**, *5*, 1558 – 1566.
[19] M. Levy, S. L. Miller, *Proc. Natl. Acad. Sci. USA* **1998**, *95*, 7933 – 7938.
[20] J. L. Bada, A. Lazcano, *Science* **2002**, *296*,1982 – 1983.
[21] O. Botta in *Astrobiology: Future Perspectives* (Eds.: P. Ehrenfreud, W. Irvine, T. Owen, L. Becker, J. Blank, J. Brucato, L. Colangeli, S. Derenne, A. Dutrey, D. Despois, A. Lazcano), Kluwer, Dordrecht, **2004**, pp. 360 – 392.
[22] T. J. Millar in *Astrobiology: Future Perspectives* (Eds.: P. Ehrenfreud, W. Irvine, T. Owen, L. Becker, J. Blank, J. Brucato, L. Colangeli, S. Derenne, A. Dutrey, D. Despois, A. Lazcano), Kluwer, Dordrecht, **2004**, pp. 17 – 21.
[23] F. J. Molster, L. B. F. M. Waters, A. G. G. M. Tielens, M. J. Barlow, *Astron. Astrophys.* **2002**, *382*, 184 – 221.
[24] L. Colangeli, Th. Henning, J. R. Brucato, D. Clément, D. Fabian, O. Guillois, F. Huisken, C. Jäger, E. K. Jessberger, A. Jones, G. Ledoux, G. Manicó, V. Mennella, F. J. Molster, H. Mutschke, V. Pirronello, C. Reynaud, J. Roser, G. Vidali, L. B. F. M. Waters, *Astron. Astrophys.* **2003**, *11*, 97 – 152.
[25] O. Botta, J. L. Bada, *Surv. Geophys.* **2002**, *23*, 411 – 467.
[26] P. G. Stocks, A. W. Schwartz, *Geochim. Cosmochim. Acta* **1982**, *46*, 309 – 315.
[27] *Kirk-Othmer Encyclopedia of Chemical Technology*, Wiley, New York, **1978**, pp. 258 – 262.
[28] H. Brederek, R. Gompper, K. Klemm, *Chem. Ber.* **1959**, *92*, 1456 – 1460.
[29] R. Gehrz in *Interstellar Dust: Proceeding of IAU Symposium 135* (Eds.: L. J. Allamandola, A. G. G. M. Tielens), Kluwer, Dordrecht, **1989**, p. 445 – 153
[30] A. P. Jones in *ASP Conference Series 122: From Stardust to Planetesimals* (Eds.: Y. J. Pendleton, A. G. G. M. Tielens), **1997**, p. 97 – 106.
[31] J. A. M. McDonnell, P. L. Lamy, G. S. Pankiewicz in *Comets in the Post Halley Era* (Eds.: R. L. Newburn, M. Neugabauer, J. Rahe), Kluwer, Dordrecht, **1991**, pp. 1043 – 1073.
[32] K. Demyk, A. P. Jones, E. Dartois, P. Cox, L. d'Hendecourt, *Astron. Astrophys.* **1999**, 394, 267 – 275.
[33] D. C. B. Whittet, A. C. A. Boogert, P. A. Gerakines, W. Schutte, A. Tielens, T. de Graauw, T. Prusti, E. F. van Dishoeck, P. R. Wesselius, C. M. Wright, *Astrophys. J.* **1997**, *490*, 729 – 734.
[34] D. E. Brownlee in *Cosmic Dust* (Ed.: A. M. McDonnell), Wiley Interscience, New York, **1978**, pp. 295 – 336.
[35] F. J. M. Rietmeijer, *Proc. 19th Lunar Planet. Sci. Conf.* **1989**, 513 – 521.
[36] F. J. M. Rietmeijer, *Rev. Mineral.* **1998**, *36*, 2 – 95.
[37] J. A. Nuth III, S. L. Hallenbeck, F. J. M. Rietmeijer in *Laboratory Astrophysics and Space Research* (Eds.: P. Ehrenfreund, K. Krafft, H. Kochan, V. Pirronello), Kluwer, Dordrecht, **1999**, pp. 143 – 182.
[38] J. R. Stephens, *Astrophys. J.* **1980**, *237*, 450 – 461.
[39] J. R. Brucato, L. Colangeli, V. Mennella, P. Palumbo, E. Bussoletti, *Astron. Astrophys.* **1999**, *348*, 1012 – 1019.
[40] *The Collected Works of J. Willard Gibbs* (Eds.: W. R. Longley, R. G. van Name), Longmans Green, New York, **1931**.
[41] C. G. Granqvist, R. A. Buhrman, *J. Appl. Phys.* **1976**, *47*, 2200 – 2219.
[42] R. Saladino, C. Crestini, F. Ciciriello, G. Costanzo, R. Negri, E. Di Mauro in *Astrobiology: Future Perspectives* (Eds.: P. Ehrenfreud, W. Irvine, T. Owen, L. Becker, J. Blank, J. Brucato, L. Colangeli, S. Derenne, A. Dutrey, D. Despois, A. Lazcano), Kluwer, Dordrecht, **2004**, pp. 393 – 413.

Received: January 27, 2005
Published online on July 8, 2005

